06

Ti−Cr−N coatings obtained by vacuum arc deposition as a basis for creating hybrid coatings

© O.I. Posylkina,[1] S.D. Latushkina,[1] I.A. Sechko,[1] A.A. Vozniakovskii,[2] E.A. Bogacheva[2]

[1] Physical Technical Institute, National Academy of Sciences of Belarus,
220141 Minsk, Belarus
[2] Ioffe Institute,
194021 St. Petersburg, Russia
e-mail: alexey_inform@mail.ru

Received October 3, 2024
Revised October 3, 2024
Accepted October 3, 2024

The results of studies of Ti−Cr−N coatings synthesized on steel substrates by vacuum-arc deposition are presented. It is established that by increasing the chromium concentration to 17 at.% it is possible to achieve an increase in microhardness up to 70% and a decrease in the friction coefficient up to 50% compared to mononitride titanium nitride coatings. The possibility of synthesis of this type of coating from cross-linked particles of few-layer graphene as the first step to create hybrid coatings is also experimentally demonstrated.

Keywords: vacuum arc deposition, friction coefficient, graphene.

DOI: 10.61011/TP.2025.02.60822.296-24

Introduction

Fabrication of coatings is one of the most widely used material surface modification techniques that provide a material with the desired properties. There are currently numerous miscellaneous coating formation techniques, for example, the electro-plasma deposition [1,2] and vacuum arc deposition method [3]. The vacuum arc deposition method is used to form homogeneous metal coatings, for example, titanium nitride and chromium nitride coatings, that feature high physical and mechanical properties [4]. Disadvantages of this method include a relatively high cost of equipment and impossibility to repair a coating without removal of the part. Therefore, researchers are increasingly using so-called hybrid coatings that consist of two or more successively deposited coatings with different functional purposes [5].

Coatings based on graphene nanostructures (GNS) are often considered as one of the components of such hybrid coatings. The reason for this are record-breaking properties of GNS: such as thermal conductivity of graphene (up to 5000 W/(m·K) [6]) and Young's modulus (up to 1 TPa [7]), etc. However, even GNS-based coatings still aren't used in manufacturing industries. The reason for this are imperfection of the coating synthesis techniques both by way of substrate-based GNS synthesis (chemical vapor deposition (CVD) [8,9], high temperature silicon carbide annealing [10,11]) and by applying pre-synthesized GNS on a substrate (spin coating, dip coating), etc. [12]). Moreover, the existing GNS synthesis techniques that are based on the „bottom–up" approach as well as on the „top–down" approach can't be used to synthesize large amounts of high quality GNS with an acceptable cost [13].

Our previous study developed a new synthesis technique for few-layer graphene ((FLG), maximum 5 cyclic-structure biopolymer layers [14]) in the self-propagating high-temperature synthesis conditions (SHS) [15], that is free from the Stone-Wales defects [16]. Possibility to synthesize large amounts of a low-cost material due to the low cost of chemicals (wood processing waste such as bark and lignin may be used as feedstock) and simplicity of equipment are an important advantage of the developed technique. Taking into account high performance of FLG together with the advantages of the SHS synthesis technique, it was assumed that the FLG particles synthesized using this approach may serve as a base material for carbon layer synthesis in hybrid coating fabrication.

The objective of this study was to fabricate the Ti−Cr−N metallic coatings with high complex of physical strength properties and to evaluate whether FLG-based coatings may be synthesized on them as the first step towards the hybrid coating fabrication.

1. Experiment

1.1. Fabrication of Ti−Cr−N-based coatings

Ti−Cr−N-based coatings were fabricated by the vacuum arc deposition method using an upgraded vacuum set equipped with two electric arc evaporators with Y-shaped system for plasma flux separation from a drop phase by means of a magnetic field. In this configuration, plasma fluxes from various sources are mixed and condensed simultaneously on a substrate, which is important for

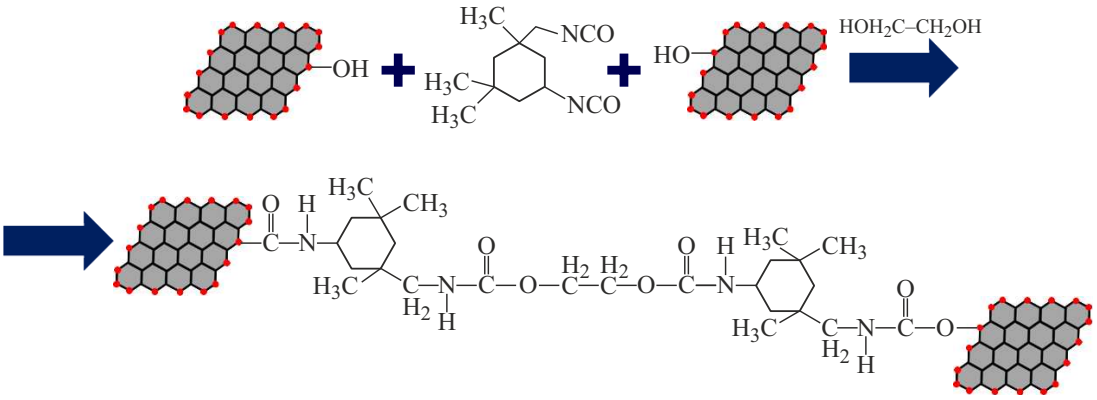

Figure 1. Flow chart of coating synthesis from FLG particles by the chemical cross-linking technique.

the multicomponent and multilayer compound synthesis. Coating were fabricated using the VT1-0 titanium and chromium cathodes, high-purity nitrogen (99.98) served as a reaction gas. Deposition in different conditions by titanium cathode current (50−100 A) and chromium cathode current (0−100 A) control was performed onto steel substrates.

1.2. Characterization of theTi−Cr−N coatings

Electronic images of the synthesized Ti−Cr−N coating were recorded by the scanning electron microscopy method using the S-4800 microscope (Hitachi, Japan). To determine the concentration of chemical elements, the quantitative Auger analysis was performed using the JXA-8500F electron probe micro-analyzer (JEOL, Norway). To avoid the substrate effect, this type of analysis used a silicon substrate. X-ray phase diffraction analysis was carried out using the DRON-3M diffractometer (Russia, copper cathode). Coating microhardness was measured by the Vickers method using the DURAMIN microhardness tester (Emco-Test, Austria) at a load of 10 g. Friction coefficient was measured using the JLTB-02 oil-free ball-on-disc tribometer (J&L Tech Co., Korea). Ball material is ShH 15, 58 . . . 63 HRC, ball load is 1 N, disk speed is 380 rpm, test time is 1 h.

1.3. Fabrication of the Ti−Cr−N/FLG hybrid coatings

Steel plates with the pre-synthesized Ti−Cr−N coatings served as a substrate for hybrid coating synthesis. To fabricate a hybrid coating, FLG particle coatings synthesized from glucose in SHS conditions were formed on the surface of the Ti−Cr−N coating [14].

Features of the SHS graphene structure formation process lead to closing of terminal valences of carbon atoms in the graphene structures by mainly oxygen-containing groups (−OH and −COOH)]. This feature was used to form cross-linked graphene structures in diisocyanate reactions. Phenols interact with isocyanates through a concerted electrophilic addition mechanism. At the same time, hydrogen-bonding-based phenol-alcohol complexes react with isocyanates through a concerted nucleophilic addition mechanism. Phenols catalyze addition of alcohols to isocyanates. Interaction between the hydrogen-bonding-based phenol-alcohol complexes and isocyanates is kinetically and thermodynamically more preferable than reactions between isocyanates and alcohol associates [17]. From these considerations, a ternary system: graphene particles/diisocyanate/diol, was developed and put into practice to form cross-linked graphene structures (graphene coatings). Reaction scheme is shown in Figure 1.

1.4. Study of resistance to hybrid coating acids

Acid resistance of hybrid coatings was studied using the following scheme: synthesized Ti−Cr−N/MG hybrid coating was brought into contact with concentrated sulfuric acid (95%, 3 ml) and held in a Petri dish for 24 h (25°C, moisture 40%).

2. Findings and discussion

Figure 2 shows a typical electronic image of the synthesized Ti−Cr−N coatings.

As shown in Figure 2, coatings are distinguished by microrelief isotropy and structure microdispersity.

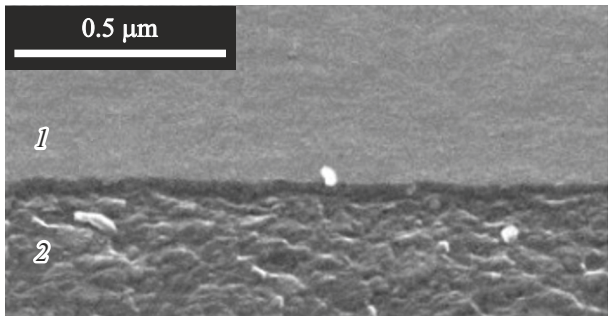

Figure 2. Electronic image of the synthesized Ti−Cr−N (17 at.% chromium) coating, plan view. *1* — initial steel substrate; *2* — Ti−Cr−N coating.

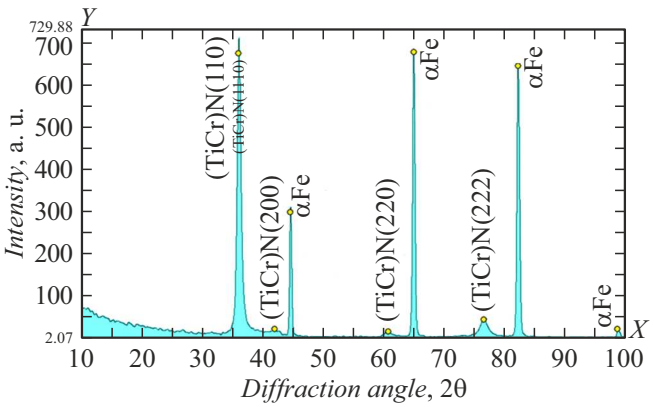

Figure 3. Diffraction pattern of the synthesized coating (17 at.% chromium) on a steel substrate.

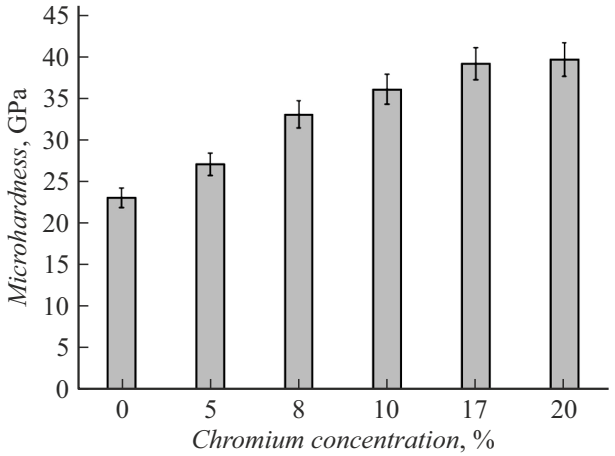

Figure 4. Dependence of the microhardness of the Ti−Cr−N coatings on the chromium concentration.

X-ray diffraction analysis was conducted to determine the phase composition of synthesized coatings. Figure 3 shows a typical diffraction pattern of the synthesized coatings.

Figure 3 shows that the recorded diffraction pattern proves the synthesis of the Ti−Cr−N coatings.

The table shows the measured content of elements in the synthesized Ti−Cr−N coatings.

Figure 4 shows the microhardness measurements of the synthesized coatings depending on the chromium concentration.

Element analysis of Ti−Cr−N coatings

Coating	Content of elements, at.%		
	Ti	Cr	N
Ti−Cr−N	32 ± 0.3	20 ± 0.3	48 ± 0.3
	28 ± 0.3	17 ± 0.3	55 ± 0.3
	32 ± 0.3	10 ± 0.3	58 ± 0.3
	32 ± 0.3	8 ± 0.3	60 ± 0.3
	37 ± 0.3	5 ± 0.3	58 ± 0.3
	38 ± 0.3	0	62 ± 0.3

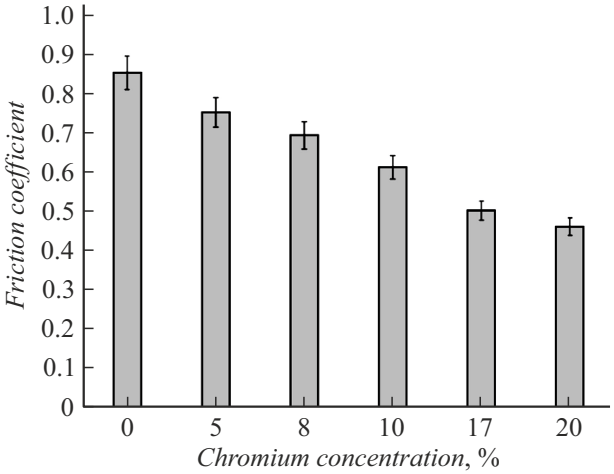

Figure 5. Dependence of the friction coefficient of the Ti−Cr−N coatings on the chromium concentration.

As shown in Figure 4, increase in the chromium concentration leads to microhardness growth up to 70% compared with mononitride titanium nitride coatings whose microhardness is not higher than 23−25 GPa [7].

Figure 5 shows the friction coefficient measurements for the Ti−Cr−N coatings depending on the chromium concentration.

As shown in Figure 5, as the chromium concentration grows, the friction coefficient decreases gradually. When the chromium concentration in the coating is 17 at.%, the friction coefficient is 50% as low as that of mononitride titanium nitride coatings. Note that further increase in the chromium concentration in the coating (up to 20 at.%) doesn't lead to further reduction of the friction coefficient any longer.

To study the microhardness and friction coefficient variation mechanism, the synthesized Ti−Cr−N coatings with different chromium concentrations were examined additionally by the X-ray diffraction method (Figure 6).

The X-ray examinations showed that the B1 NaCl structure is typical of the Ti−Cr−N coatings. The Ti−Cr−N coatings have a strongly pronounced reflection intensity in the (111) lattice plane orientation, and this intensity becomes much lower as the chromium concentration increases (Figure 6). The Ti−Cr−N lattice spacing decreases as the chromium concentration grows (0.4313 nm with 5 at.% chromium to 0.4217 nm with 17 at.% chromium). Chromium concentration growth in the Ti−Cr−N coatings leads to formation of (Ti,Cr)N-based solid solution with 10 nm coherent scattering areas with a lower reflection intensity from the (111) lattice planes, which may cause both the microhardness growth and friction coefficient reduction.

The next work step was to identify whether a coating may be synthesized from the cross-linked FLG particles on the Ti−Cr−N coating. Using the obtained dependence of the Ti−Cr−N coating properties on the chromium

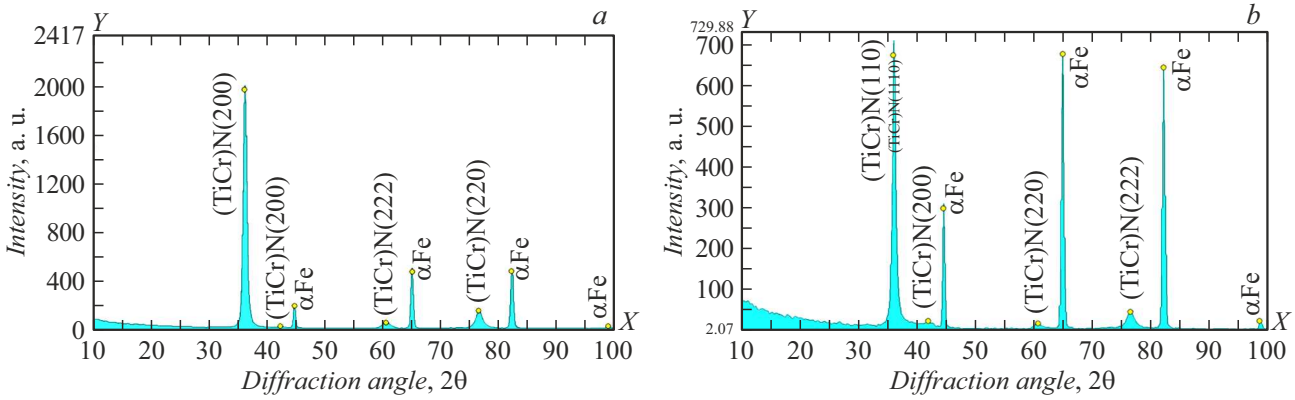

Figure 6. Diffraction patterns of the Ti−Cr−N coatings. *a* — 5; *b* — 17 at.% chromium.

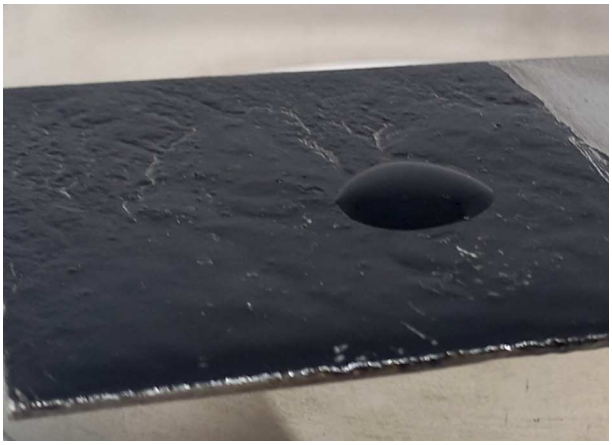

Figure 7. Photograph of the Ti−Cr−N coating (17 at.% chromium) with the deposited FLG particle coating after the contact with sulfuric acid during 24 h.

concentration, a Ti−Cr−N sample with 17 at.% chromium was chosen for further work..

Figure 7 shows a photograph of a Ti−Cr−N (17 at.%)/FLG coating with a deposited FLG particle coating during the acid resistance test.

As shown in Figure 7, the Ti−Cr−N coatings may serve as a substrate for the synthesis of cross-linked FLG particle coatings. During 24 h, the acid didn't react with the Ti−Cr−N layer, which can be seen by the absence of chemical reaction signs — absence of oxides and a constant acid volume.

Conclusion

It was found that the Ti−Cr−N coatings synthesized by the vacuum arc deposition method were much better than mononitride titanium nitride coatings in microhardness and friction coefficient due to formation of (Ti,Cr)N-based solid solution. It was also shown experimentally that these coatings were suitable as a substrate for formation of cross-linked few-layer graphene particle coatings to form hybrid coatings, which may provide a synergistic effect. Future studies will investigate a set of physical and mechanical, electrophysical and thermophysical properties of such hybrid coatings.

Funding

The study was supported by grants of the Belarusian Republican Foundation for Fundamental Research№ T23RNFM and RNF 24-49-10014.

Conflict of interest

The authors declare no conflict of interest.

References

[1] V.A. Koshuro, G.G. Nechaev, A.V. Lyasnikova. Tech. Phys., **59** (10), 1570 (2014). DOI: 10.1134/S106378421410020X
[2] A.V. Lyasnikova, S.Y. Pichkhidze, O.A. Dudareva, O.A. Markelova. Tech. Phys., **60** (11), 1725 (2015). DOI: 10.1134/S1063784215110183
[3] A.D. Pogrebnjak, I.V. Yakushchenko, O.V. Bondar, M.A. Lisovenko, O.V. Sobol', V.M. Beresnev, A.I. Kupchishin, H. Amekura, K. Kono, K. Oyoshi, Y. Takeda. Tech. Phys., **60** (8), 1176 (2015). DOI: 10.1134/S1063784215080228
[4] B. Fotovvati, N. Namdari, A. Dehghanghadikolaei. J. Manuf. Mater. Process., **3** (1), 28 (2019). DOI: 10.3390/jmmp3010028
[5] M.H. Nazari, Y. Zhang, A. Mahmoodi, G. Xu, J. Yu, J. Wu, X. Shi. Prog. Org. Coat., **162**, 106573 (2022). DOI: 10.1016/j.porgcoat.2021.106573
[6] A.A. Balandin, S. Ghosh, W. Bao, I. Calizo, D. Teweldebrhan, F. Miao, C.N. Lau. Nano Lett., **8** (3), 902 (2008). DOI: 10.1021/nl0731872
[7] A.R. Urade, I. Lahiri, K.S. Suresh. Jom., **75** (3), 614 (2023). DOI: 10.1007/s11837-022-05505-8
[8] N.A. Nebogatikova, I.V. Antnova, R.A. Soots, K.A. Kokh, E.S. Klimova, V.A. Volodin. ZhTF, **92** (4), 261 (2024). (in Russian) DOI: 10.61011/JTF.2024.02.57081.281-23

[9] A.B. Loginov, R.R. Ismagilov, A.N. Obraztsov, I.V. Bozhev, S.N. Bokova-Sirosh, E.D. Obraztsova, B.A. Loginov. Tech. Phys., **64** (11), 1666 (2019). DOI: 10.1134/S1063784219110185
[10] S.P. Lebedev, S.Iu. Priobrazhenskii, A.V. Plotnikov, M.G. Mynbaeva, A.A. Lebedev. Tech. Phys., **68** (12), 648 (2022). DOI: 10.1134/S1063784223080169
[11] S.P. Lebedev, I.S. Barash, I.A. Eliseyev, P.A. Dementev, A.A. Lebedev, P.V. Bulat. Tech. Phys., **64** (12), 1843 (2019). DOI: 10.1134/S1063784219120144
[12] O. Kwon, Y. Choi, E. Choi, M. Kim, Y.C. Woo, D.W. Kim. Nanomaterials, **11** (3), 757 (2021). DOI: 10.3390/nano11030757
[13] X. Gu, Y. Zhao, K. Sun, C.L. Vieira, Z. Jia, C. Cui, Z. Wang, A. Walsh, S. Huang. Ultrason. Sonochem., **58**, 104630 (2019). DOI: 10.1016/j.ultsonch.2019.104630
[14] *Nanotechnologies — Structural characterization of graphene — Part 1: Graphene from powders and dispersions* ISO/TS 21356-1
[15] A.P. Voznyakovskii, A.A. Vozniakovskii, S.V. Kidalov. Nanomaterials, **12** (4), 657 (2022). DOI: 10.3390/nano12040657
[16] A.P. Voznyakovskii, A.A. Neverovskaya, A.A. Vozniakovskii, S.V. Kidalov. Nanomaterials, **12** (5), 883 (2022). DOI: 10.3390/nano12050883
[17] S.V. Nesterov. *Vliyanie fenolnykh soedinenii na protsess obrazovaniya poliuretanov i ikh termicheskuiyu stabilnost* (Avtoref. diss., 2013)

Translated by E.Ilinskaya